Supporting Information

Facile Synthesis of Heterogeneous Macrocycles for Intramolecular Energy Transfer

Ao Liu[+,a] *Xin Meng*[+,a] *Chen-Chen Shen,*[a] *Zhi-Yuan Zhang,*[a] *and Chunju Li* [*, a]

§. Tianjin Key Laboratory of Structure and Performance for Functional Molecules, College of Chemistry, Tianjin Normal University, Tianjin 300387 (P. R. China).

Corresponding Author

*E-mail: cjli@shu.edu.cn

Table of Contents

Section I. Materials/Methods/Instrumentation 2

Section II. Synthetic Protocols of MOH T1OH T2OH T3OH. 3-17

Section III. Photophysical Properties of T T1OH T2OH T3OH 18-24

Section IV. References 25

Section I. Materials/Methods/Instrumentation

All reagents and solvents were commercially available and used without further purification, unless otherwise noted. ^{1}H and ^{13}C NMR spectra were recorded on Bruker Avance III 400 MHz. High-resolution mass spectra (HRMS) were determined on Bruker Daltonics Inc. APEXIII 7.0 TESLA FTMS. Melting points were obtained on an X-4 digital melting point apparatus without correction. The single crystal X-ray data were measured by direct methods using Bruker D8 VENTURE and Bruker SMARE APEX II. UV-Vis titration and UV-Vis were received by Agilent Cary 100 UV-Vis. Fluorescence spectra and lifetimes were measured on FLS1000. Fluorescence quantum efficiencies were measured on HAMAMATSU C9920-02 by absolute method.

The geometry optimization of **T2OH** and **T3OH** were performed by using Mopac2016 program[1] with PM7[2] level.

Section II. Synthetic Protocols.

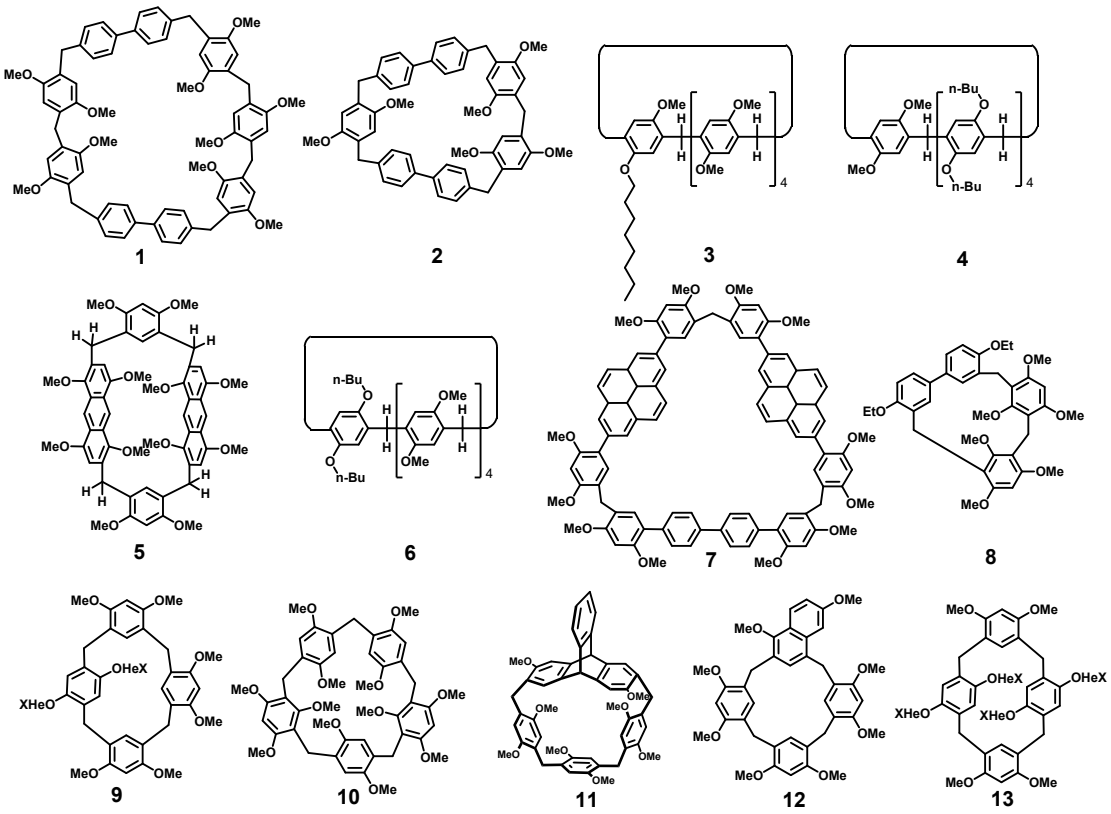

Figure S1. The structures of reported heterogeneous macrocyclic arenes.

Table S1. The yields of reported heterogeneous macrocyclic arenes and our works.

Entry	Name	Yields (%)	References
1	**1**	0.1	[4]
2	**2**	0.1	[4]
3	**3**	9	[5]
4	**4**	9	[7]
5	**5**	10	[6]
6	**6**	16	[7]
7	**7**	24	[8]
8	**8**	25	[9]
9	**9**	26	[10]
10	**10**	35	[10]
11	**11**	37	[11]
12	**12**	47	[12]
13	**13**	53	[10]
14	**T1OH**	43	This work
15	**T2OH**	31	This work
16	**T3OH**	94	This work

17	**T1OH, T2OH, T3OH**	33, 26, 30	This work

The first compounds **T** and **M** were synthesized by using the method from the reference.[13]

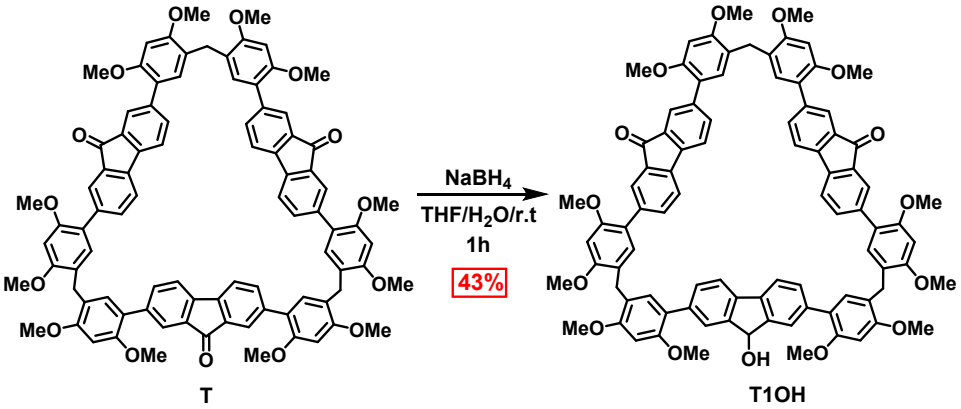

Scheme S1. Synthesis of heterogeneous macrocycle **T1OH**.

T1OH. To a solution of **T** (0.30 g, 0.22 mmol) in 150 mL THF and 5 mL water (30:1) was added $NaBH_4$ (12 mg, 0.32 mmol) that was dispersed in 5 mL THF and stirred at 25 ℃ for 1 h. After quenching with water and extracting with CH_2Cl_2, the solvents was removed under vacuum, and the residue was purified by column chromatography (silica gel, eluent: ethyl acetate/CH_2Cl_2 1:60) to afford product **T1OH** as an orange solid (0.13 g, 43 %). M. p. 261-262 ℃. ^{1}H NMR (400 MHz, $CDCl_3$, ppm): δ 7.75 (d, J = 6.2 Hz, 6H), 7.60 (dd, J = 7.7, 1.6 Hz, 2H), 7.45 (td, J = 16.2, 8.4, 4.9 Hz, 12H), 7.00 (d, J = 1.2 Hz, 1H), 6.92 (s, 3H), 6.60 – 6.54 (m, 6H), 5.62 (s, 1H), 3.92 (s, 6H), 3.90 (s, 18H), 3.83 (s, 18H); ^{13}C NMR (100 MHz, $CDCl_3$, ppm): δ 194.61 (s), 158.24 (d, J = 4.0 Hz), 157.94 (s), 155.93 (d, J = 9.1 Hz), 145.82 (s), 142.54 (s), 139.49 (d, J = 6.8 Hz), 138.36 (s), 138.02 (s), 135.60 (d, J = 8.5 Hz), 134.48 (d, J = 5.0 Hz), 132.20 (s), 131.53 (d, J = 10.5 Hz), 130.31 (s), 126.34 (s), 125.62 (d, J = 5.1 Hz), 122.70 (s), 121.42 (dd, J = 27.4, 19.2 Hz), 120.02 (d, J = 5.6 Hz), 119.57 (s), 96.11 (s), 95.87 (s), 56.26 – 55.85 (m), 27.77 (s). HRMS (m/z): calcd. for $C_{90}H_{74}O_{15}^+$: 1394.5028 $[M]^+$; found, 1394.5015 $[M]^+$.

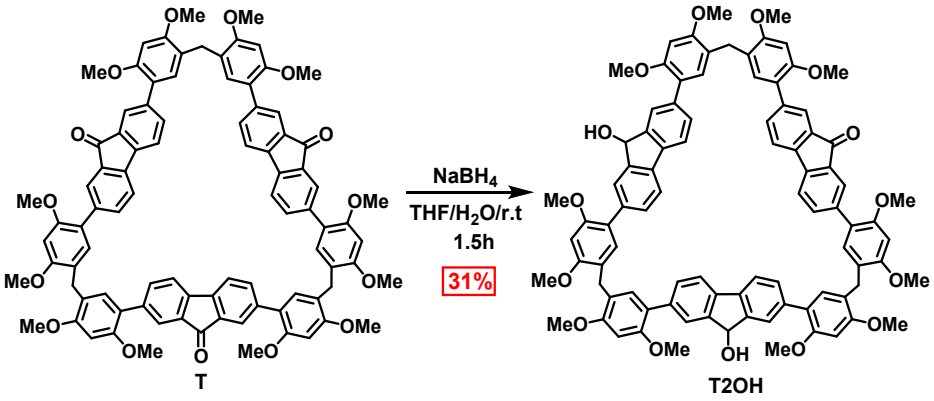

Scheme S2. Synthesis of heterogeneous macrocycle **T2OH**.

T2OH. To a solution of **T** (0.30 g, 0.22 mmol) in 150 mL THF and 5 mL water (30:1) was added $NaBH_4$ (20 mg, 0.53 mmol) and stirred at 25 ℃ for 90 minutes. After quenching with water and extracting with CH_2Cl_2, the solvents was removed under vacuum, and the residue was purified by column chromatography (silica gel, eluent: ethyl acetate/CH_2Cl_2 1:60 and gradually changed to ethyl acetate/CH_2Cl_2 1:30) to afford **T2OH** as an orange solid (93 mg, 31 %). M. p. 267-269 ℃. ^{1}H NMR (400 MHz, $CDCl_3$, ppm) : δ 7.73 (d, J = 9.1 Hz, 6H), 7.59 (d, J = 7.7 Hz, 4H), 7.49 (d, J = 7.7 Hz, 2H), 7.46 – 7.40 (m, 6H), 6.97 (d, J = 10.8 Hz, 4H), 6.90 (s, 2H), 6.60 – 6.55 (m, 6H), 5.61 (d, J = 4.7 Hz, 2H), 3.93 (d, J = 4.9 Hz, 6H), 3.90 (s, 18H), 3.84 (d, J = 4.2 Hz, 18H); ^{13}C NMR (100 MHz, $CDCl_3$, ppm): δ 194.59 (s), 158.28 (s), 157.98 (d, J = 3.7 Hz), 155.98 (d, J = 10.1 Hz), 145.82 (d, J = 7.5 Hz), 142.56 (s), 139.58 (s), 138.37 (s), 138.12 (d, J = 6.5 Hz), 135.64 (s), 134.55 (s), 132.21 (d, J = 11.5 Hz), 131.52 (s), 130.39 (d, J = 7.9 Hz), 126.33 (d, J = 5.4 Hz), 125.60 (s), 122.78 (s), 121.75 (s), 121.54 (d, J = 2.1 Hz), 121.25 (s), 119.94 (s), 119.53 (d, J = 6.0 Hz), 96.52 – 96.34 (m), 96.09 (d, J = 23.4 Hz), 56.37 – 55.84 (m), 27.84 (s). HRMS (m/z): calcd. for $C_{90}H_{76}O_{15}^+$: 1396.5184 $[M]^+$; found, 1396.5181 $[M]^+$.

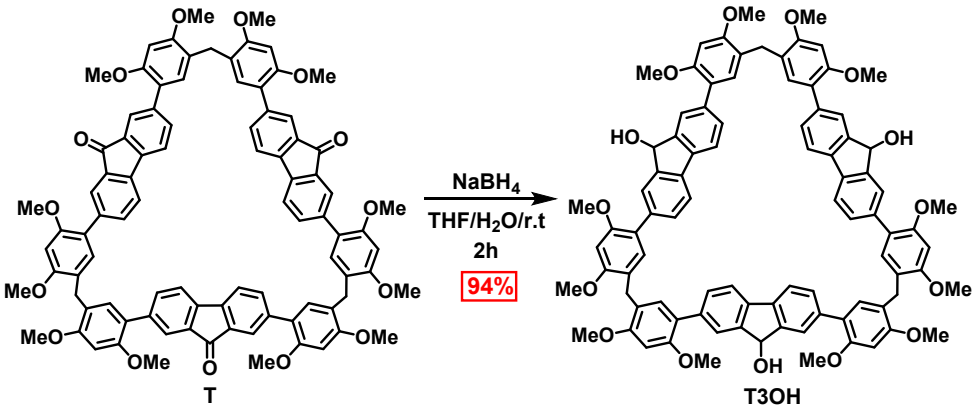

Scheme S3. Synthesis of macrocycle **T3OH**.

T3OH. To a solution of **T** (0.30 g, 0.22 mmol) in 30 mL THF and 1 mL water (30:1) was added $NaBH_4$ (0.17 g, 4.5 mmol) and stirred at 25 ℃ for 2 h. After quenching with water and extracting with CH_2Cl_2, the solvents was removed under vacuum, and the residue was purified by column chromatography (silica gel, eluent: ethyl acetate/CH_2Cl_2 1:20) to afford product **T3OH** as a yellow solid (0.28 g, 94 %). M. p. 281-283 ℃. ^{1}H NMR (400 MHz, $CDCl_3$): δ 7.71 (s, 6H), 7.58 (d, J = 7.8 Hz, 6H), 7.43 (d, J = 7.9 Hz, 6H), 6.97 (s, 6H), 6.58 (s, 6H), 5.60 (d, J = 5.0 Hz, 3H), 3.94 (s, 6H), 3.90 (s, 18H), 3.83 (s, 18H); ^{13}C NMR (100 MHz, $CDCl_3$, ppm): δ 157.94, 155.88, 145.76, 138.33, 138.12, 132.14, 130.41, 126.27, 122.65, 121.42, 121.39, 119.48, 96.04, 56.10, 55.98, 27.87. HRMS (m/z): calcd. for $C_{90}H_{78}O_{15}^+$: 1398.5341 $[M]^+$; found, 1398.5341 $[M]^+$.

Table S2. Screening of reaction conditions for heterogeneous macrocycles by post-modification.

Entry	$NaBH_4$ (equiv) [a]	Reaction time (min)	Yields (%) **T1OH**	Yields (%) **T2OH**	Yields (%) **T3OH**
1	1	10	5	2	-[b]
2	1	20	10	2	1
3	1	60	10	1	2

4	1.5	30	20	6	5
5	1.5	60	43	10	8
6	1.5	90	30	19	11
7	2.5	30	24	9	9
8	2.5	60	38	27	10
9	2.5	90	22	31	20
10	2.5	120	16	23	34
11	3	30	25	11	18
12	3	60	33	26	30
13	3	90	21	20	48
14	5	90	19	13	46
15	5	120	10	6	62
16	5	240	3	2	76
17	10	60	10	3	63
18	10	120	4	2	75
19	10	240	1	1	90
20	20	60	6	4	84
21	20	120	0	0	94
22	20	180	0	0	94

a: The reductant is $NaBH_4$ and solvent is THF/ H_2O (30: 1) which is the optimal condition for the reduction of fluorenone.[3] b: Not detected.

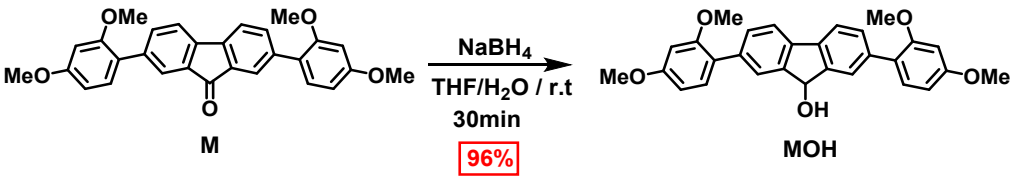

Scheme S4. Synthesis of monomer **MOH**.

MOH. To a solution of **M** (0.50 g, 1.1 mmol) in 90 mL THF and 3 mL water (30:1) was added $NaBH_4$ (0.13 g, 4.4 mmol) and stirred at 25 ℃ for 30 minutes. After quenching with water and extracting with CH_2Cl_2, the solvents was removed under vacuum to afford the product **MOH** as a white solid (0.48 g, 96 %).[1] M. p. 182-183 ℃. ^{1}H NMR (400 MHz, DMSO-d_6, ppm): δ 7.75 (d, J = 7.9 Hz, 2H), 7.64 (s, 2H), 7.45 (dd, J = 7.8, 1.3 Hz, 2H), 7.27 (d, J = 8.4 Hz, 2H), 6.69 (d, J = 2.3 Hz, 2H), 6.64 (dd, J = 8.4, 2.4 Hz, 2H), 5.84 (s, 1H), 5.53 (s, 1H), 3.82 (s, 6H), 3.79 (s, 6H); ^{13}C NMR (100

MHz, DMSO-d_6, ppm): δ 160.05, 157.20, 146.87, 137.53, 137.14, 130.86, 129.40, 125.77, 122.62, 119.35, 105.35, 99.01, 73.66, 55.60, 55.29. calcd. for $C_{29}H_{26}O_5^+$: 454.1780 $[M]^+$; found, 454.1773 $[M]^+$.

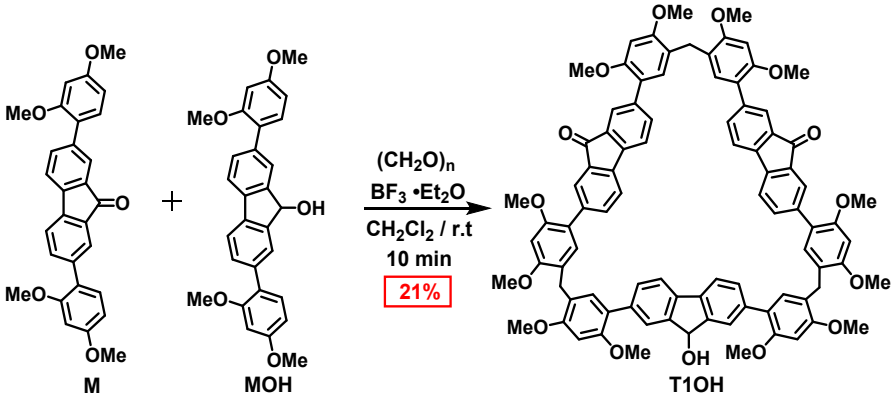

Scheme S5. Synthesis of macrocycle **T1OH**.

T1OH. A mixture of **M** (0.40 g, 0.88 mmol), **MOH** (0.20 g, 0.44 mmol) and paraformaldehyde (0.30 g, 10 mmol) in CH_2Cl_2 (100 mL) was added boron trifluoride diethyl etherate (0.60 mL, 5.07 mmol) and stirred at 25 ℃ for 10 minutes. After quenching by 50 mL water, the water phase was removed and washed with saturated $NaHCO_3$ solution two times. Remove the water in the organic phase through anhydrous sodium sulfate and evaporated. The residue was purified by column chromatography on silica gel (ethyl acetate/CH_2Cl_2 1:60) to afford **T1OH** (43 mg, 21 %).

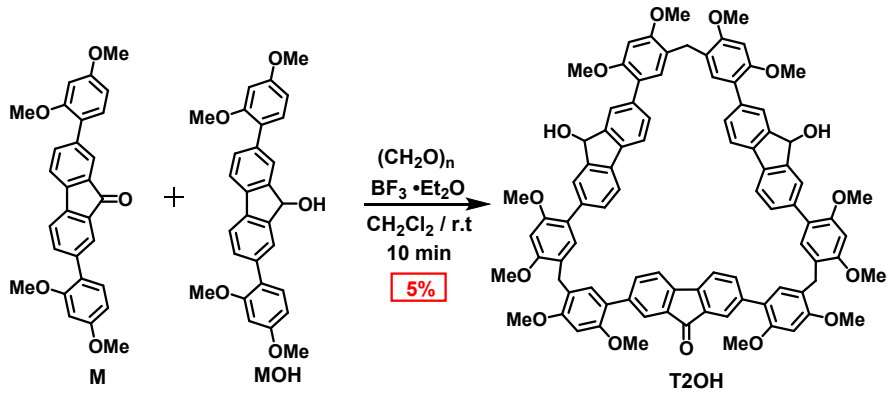

Scheme S6. Synthesis of macrocycle **T2OH**.

T2OH. To the solution of **M** (0.20 g, 0.44 mmol)、**MOH** (0.40 g, 0.88 mmol) and paraformaldehyde(0.30 g,10 mmol) in DCM (100 mL) was added boron trifluoride diethyl etherate (0.60 mL, 5.1 mmol) and stirred at 25 ℃ for 10 minutes. After quenching by 50 mL water, the water phase was removed and washed with saturated $NaHCO_3$ solution two times. Remove the water in the organic phase through anhydrous sodium sulfate and evaporated. The residue was purified by column chromatography on silica gel (ethyl acetate/CH_2Cl_2 1:30 to afford **T2OH** (10 mg, 5.0 %).

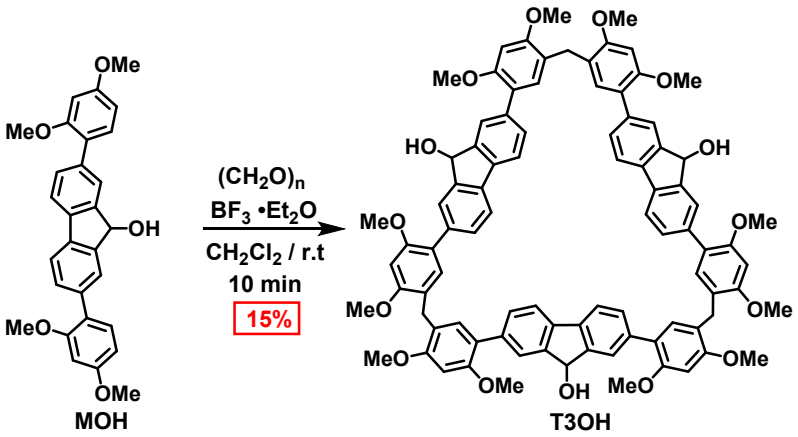

Scheme S7. Synthesis of macrocycle **T3OH**.

T3OH. To the solution of **MOH** (0.40 g, 0.88 mmol) and paraformaldehyde (0.30 g,10 mmol) in DCM (100 mL) was added boron trifluoride diethyl etherate (0.60 mL, 5.1 mmol) and stirred at 25 ℃ for 10 minutes. After quenching by 50 mL water, the water phase was removed and washed with saturated $NaHCO_3$ solution two times. Remove the water in the organic phase through anhydrous sodium sulfate and evaporated. The residue was purified by column chromatography on silica gel (silica gel, eluent: ethyl acetate/CH_2Cl_2 1:20) to afford **T3OH** (60 mg, 15 %).

Table S3. Screening of reaction conditions for heterogeneous macrocycles by one-pot co-cyclization.

Entry	M (equiv)	MOH (equiv)	Catalysts	Reaction time (min)	Yields(%) T1OH	Yields(%) T2OH	Yields(%) T3OH
1	2	1	BF_3•Et_2O	5	12	1	0
2	2	1	BF_3•Et_2O	10	21	3	0.1
3	2	1	BF_3•Et_2O	20	11	2	0.1
4	1	2	BF_3•Et_2O	5	1	2	0.1
5	1	2	BF_3•Et_2O	10	2	5	1
6	1	2	BF_3•Et_2O	20	1	2	0.5
5	0	3	BF_3•Et_2O	5	0	0	8
6	0	3	BF_3•Et_2O	10	0	0	15
7	0	3	BF_3•Et_2O	20	0	0	9
8	2	1	CF_3SO_3H	1	-[a]	-[a]	-[a]
9	2	1	$FeCl_3$	60	-[b]	-[b]	-[b]
10	2	1	$AlCl_3$	60	-[b]	-[b]	-[b]

a: Only polymer was found. b: Not react.

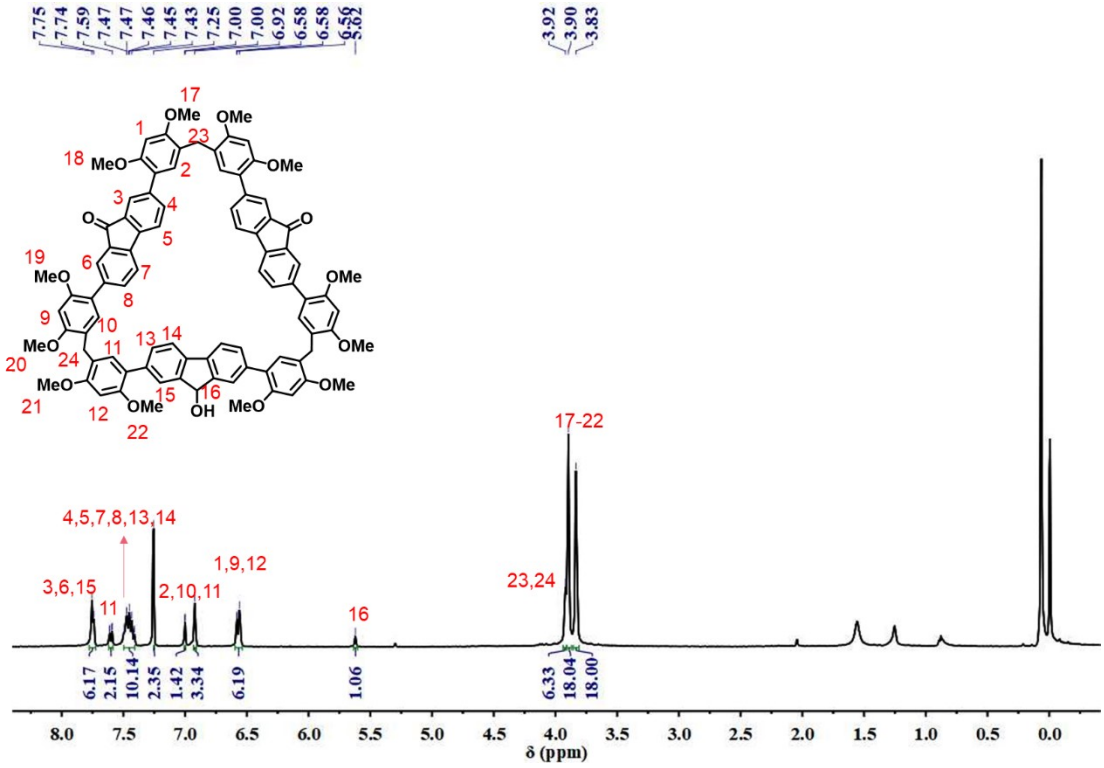

Figure S2. ^{1}H NMR spectrum (400 MHz, $CDCl_3$, 298K) of **T1OH**.

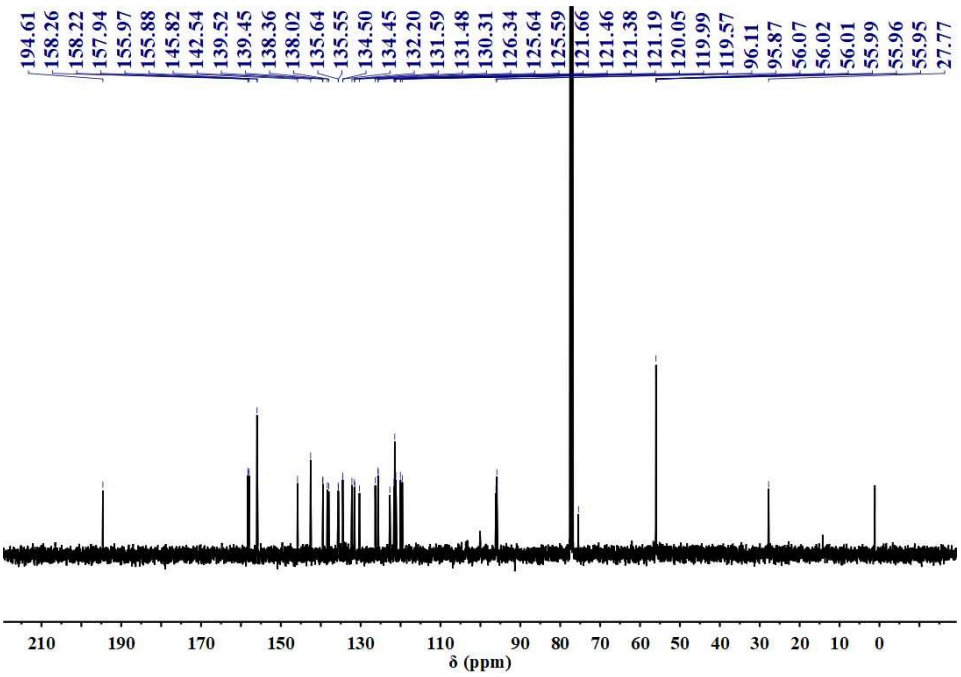

Figure S3. ^{13}C NMR spectrum (100 MHz, $CDCl_3$, 298K) of **T1OH**.

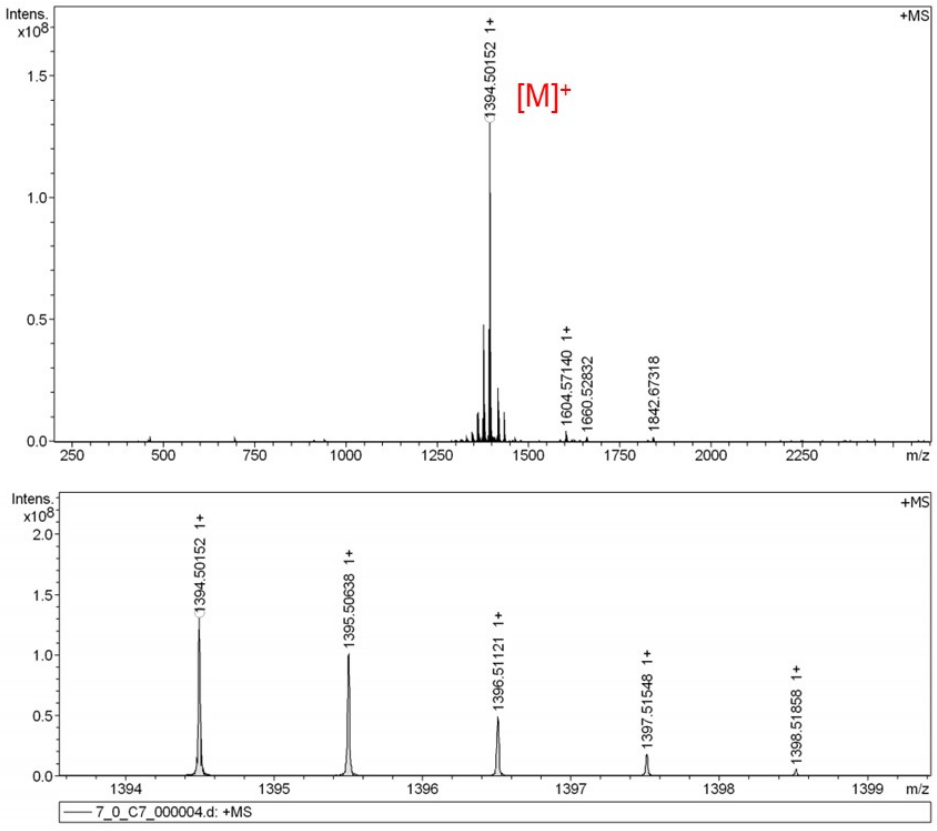

Meas. m/z	#	Ion Formula	Score	m/z	err [ppm]	Mean err [ppm]	mSigma	rdb	e⁻ Conf	N-Rule
1394.501518	1	C90H74O15	100.00	1394.502223	0.5	-0.4	103.9	54.0	odd	ok

Figure S4. HRMS of **T1OH**.

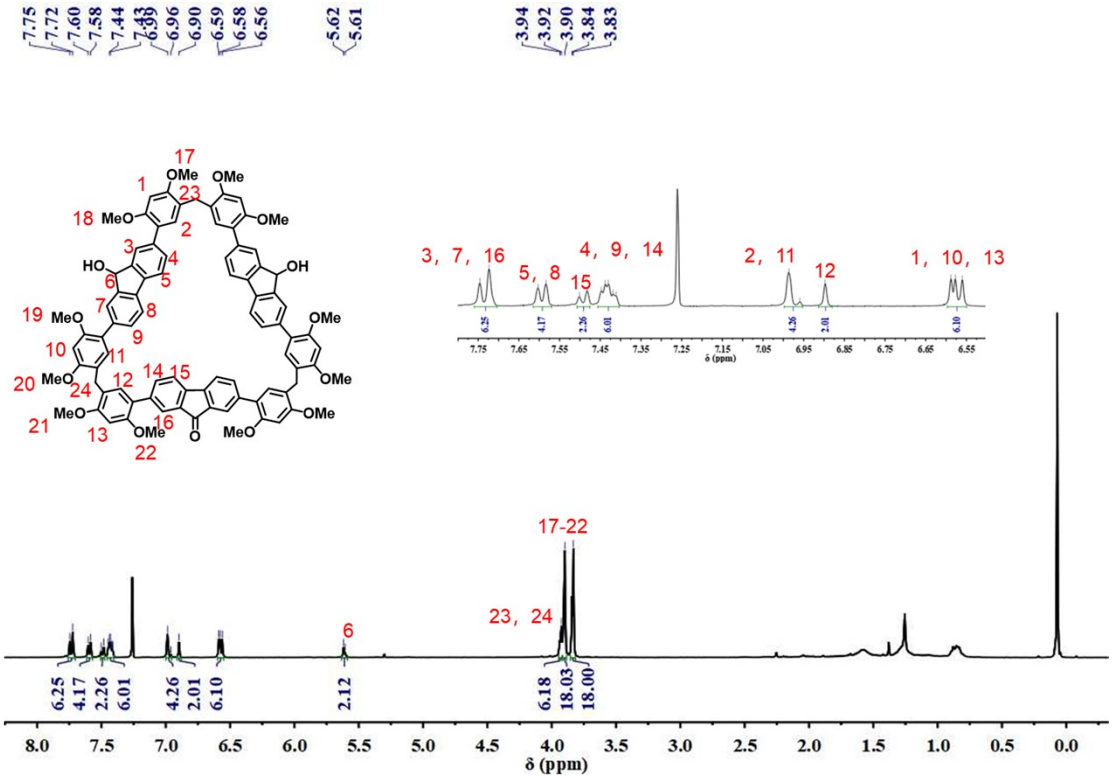

Figure S5. ^{1}H NMR spectrum (400 MHz, $CDCl_3$, 298K) of **T2OH**.

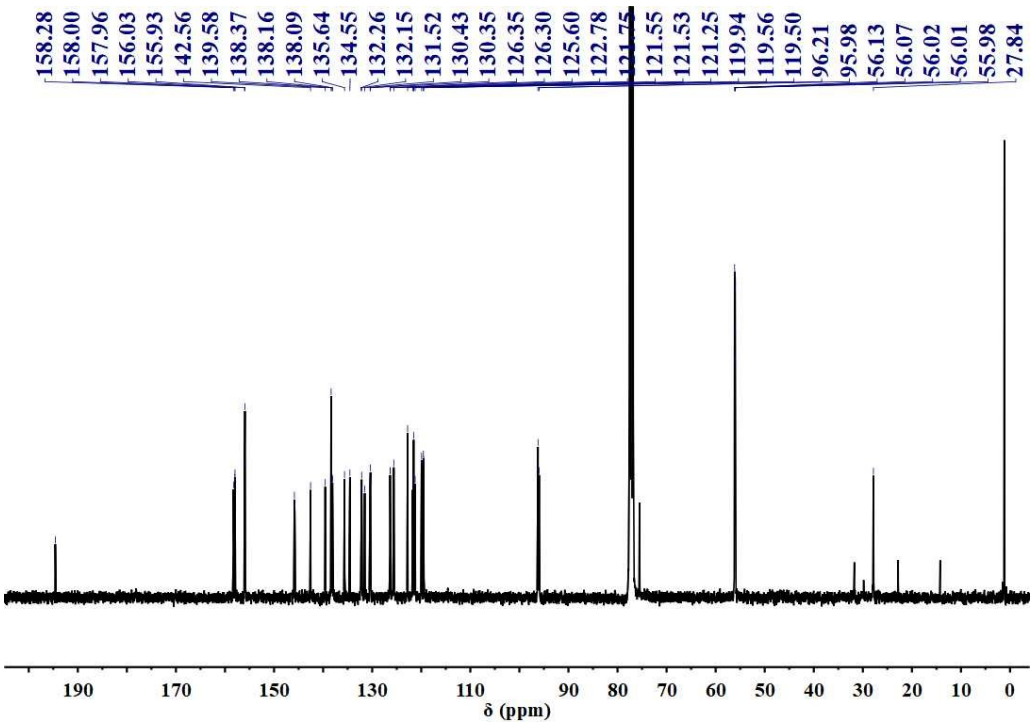

Figure S6. ^{13}C NMR spectrum (100 MHz, $CDCl_3$, 298K) of **T2OH**.

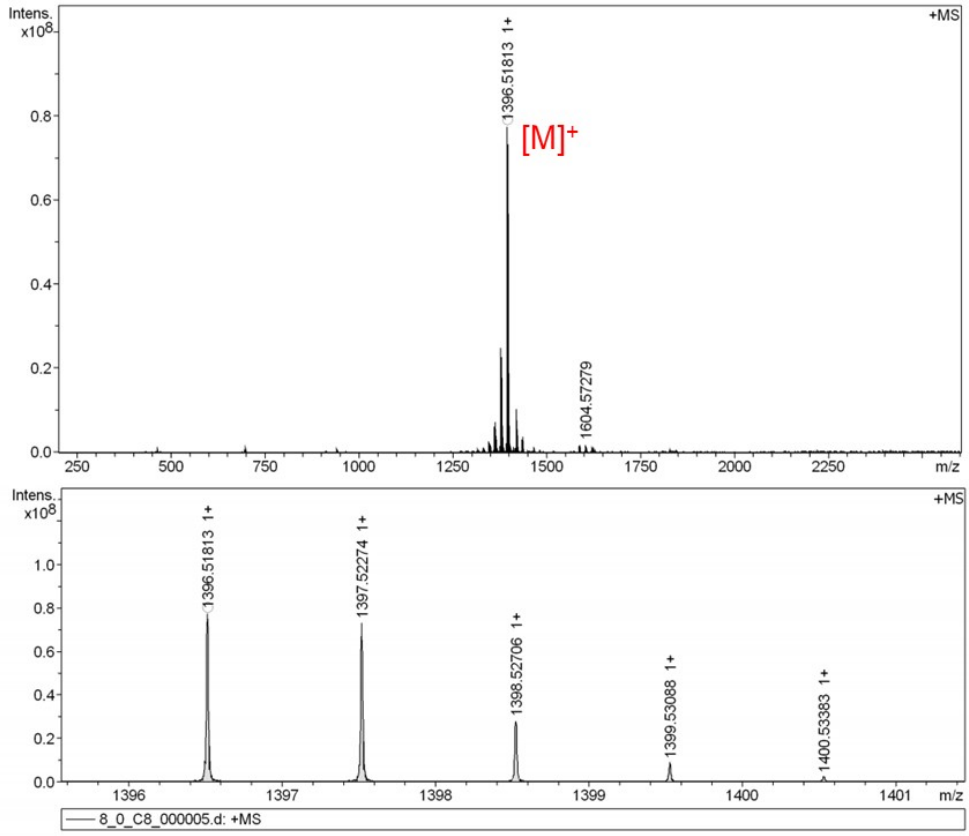

Meas. m/z	#	Ion Formula	Score	m/z	err [ppm]	Mean err [ppm]	mSigma	rdb	e⁻ Conf	N-Rule
1396.518126	1	C90H76O15	100.00	1396.517873	0.2	-0.9	72.3	53.0	odd	ok

Figure S7. HRMS of **T2OH**.

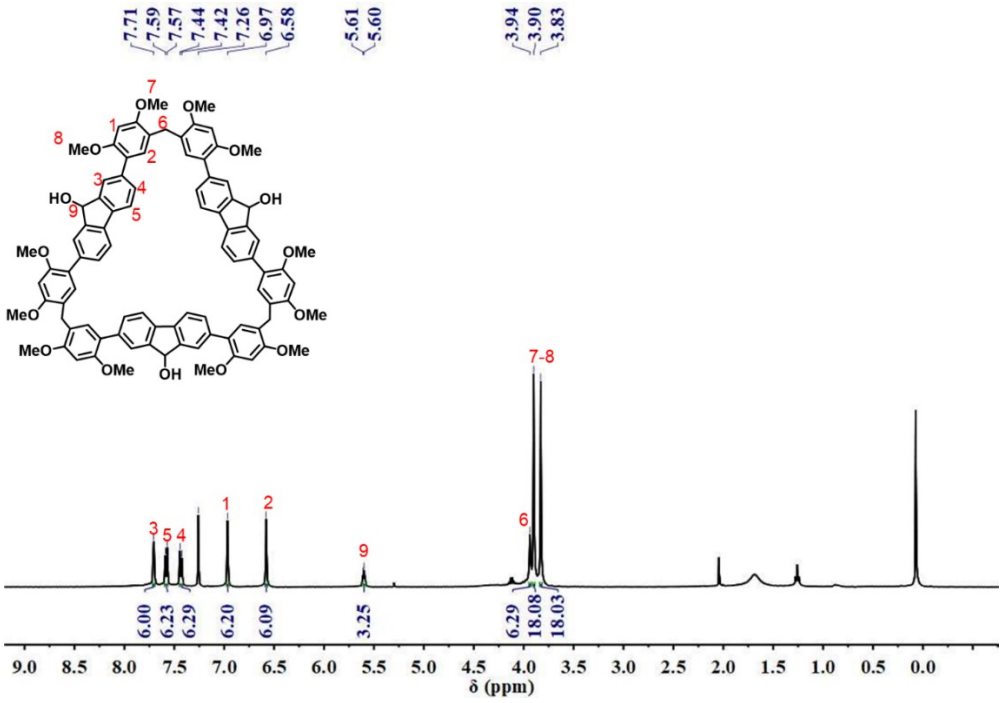

Figure S8. ^{1}H NMR spectrum (400 MHz, $CDCl_3$, 298K) of **T3OH**.

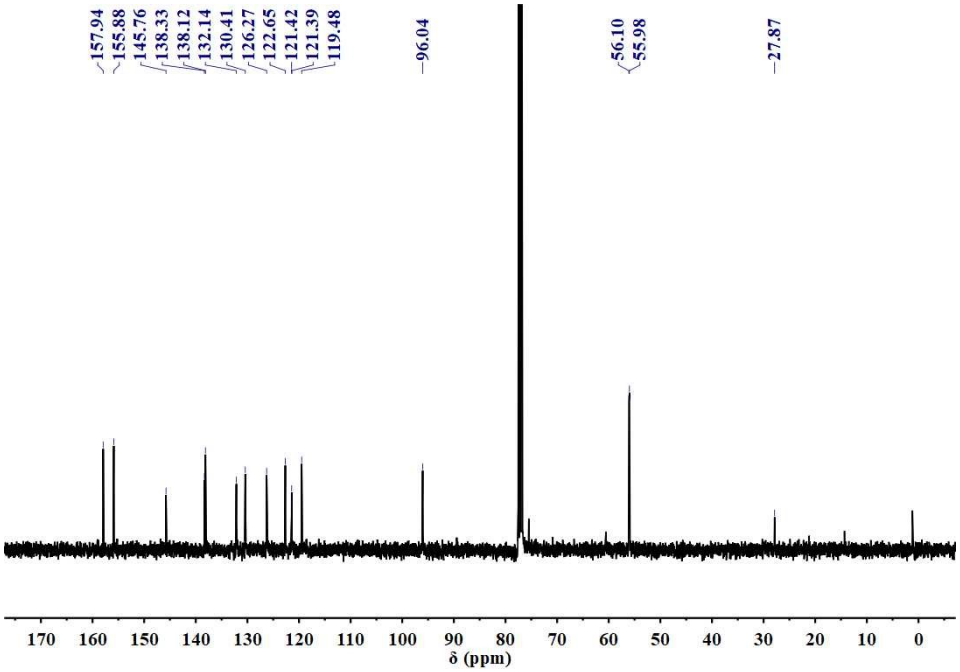

Figure S9. ^{13}C NMR spectrum (100 MHz, $CDCl_3$, 298K) of **T3OH**.

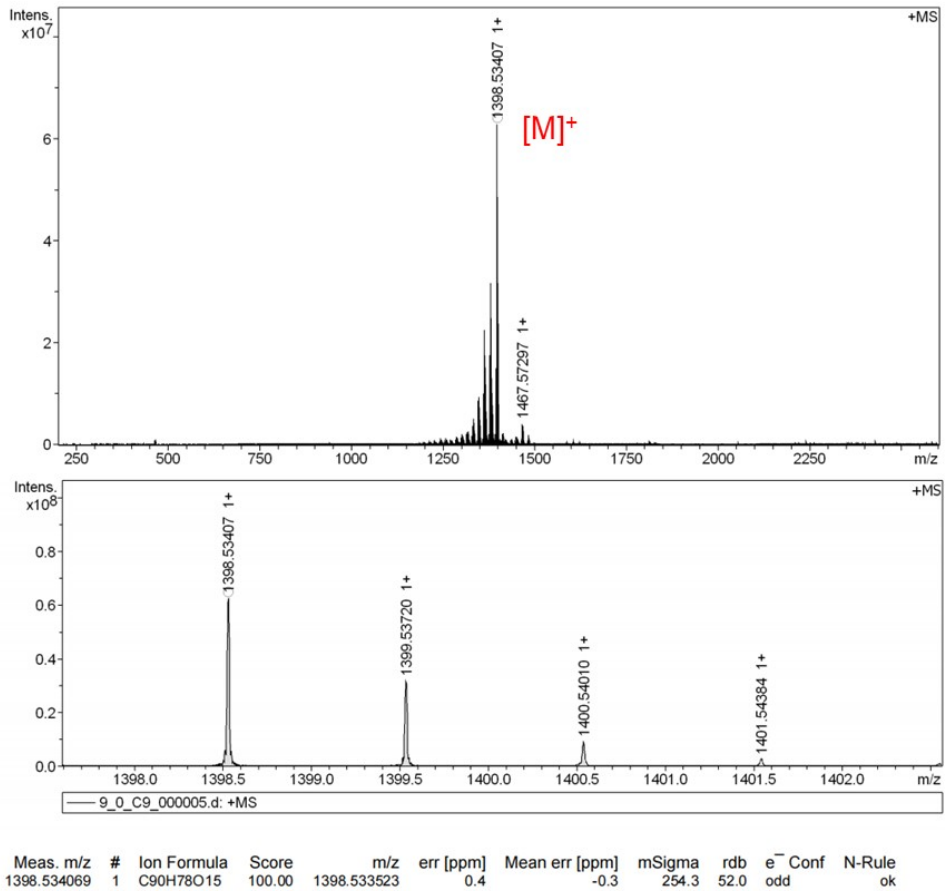

Meas. m/z	#	Ion Formula	Score	m/z	err [ppm]	Mean err [ppm]	mSigma	rdb	e⁻ Conf	N-Rule
1398.534069	1	C90H78O15	100.00	1398.533523	0.4	-0.3	254.3	52.0	odd	ok

Figure S10. HRMS of **T3OH**.

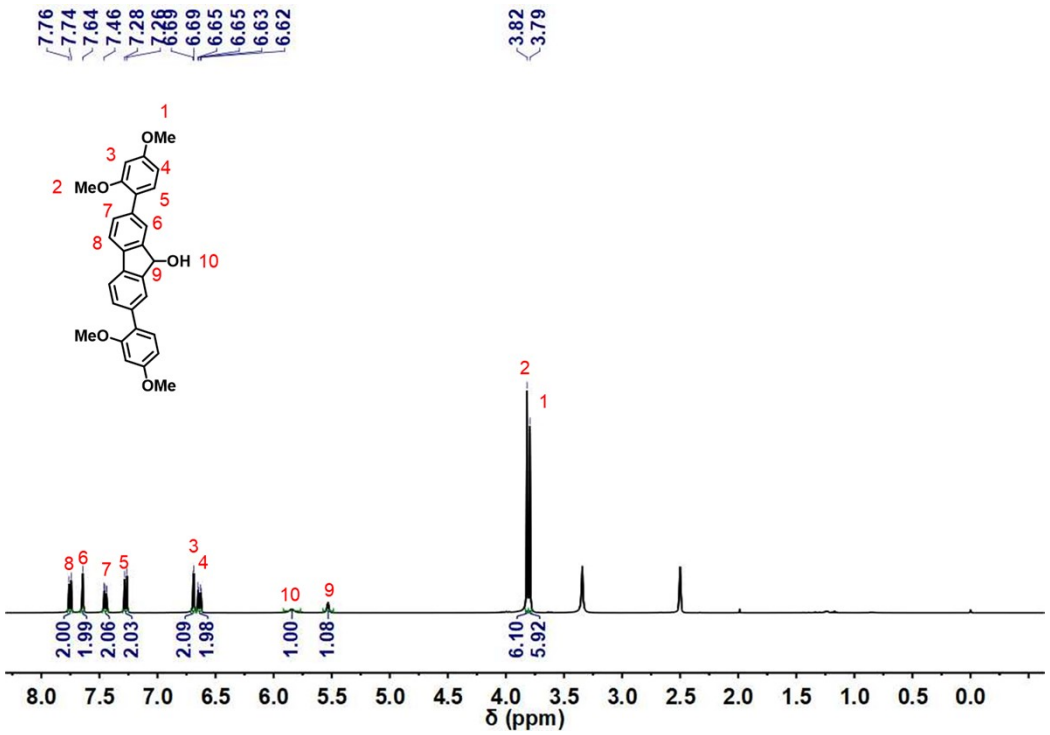

Figure S11. [1]H NMR spectrum (400 MHz, DMSO-d_6, 298K) of **MOH**.

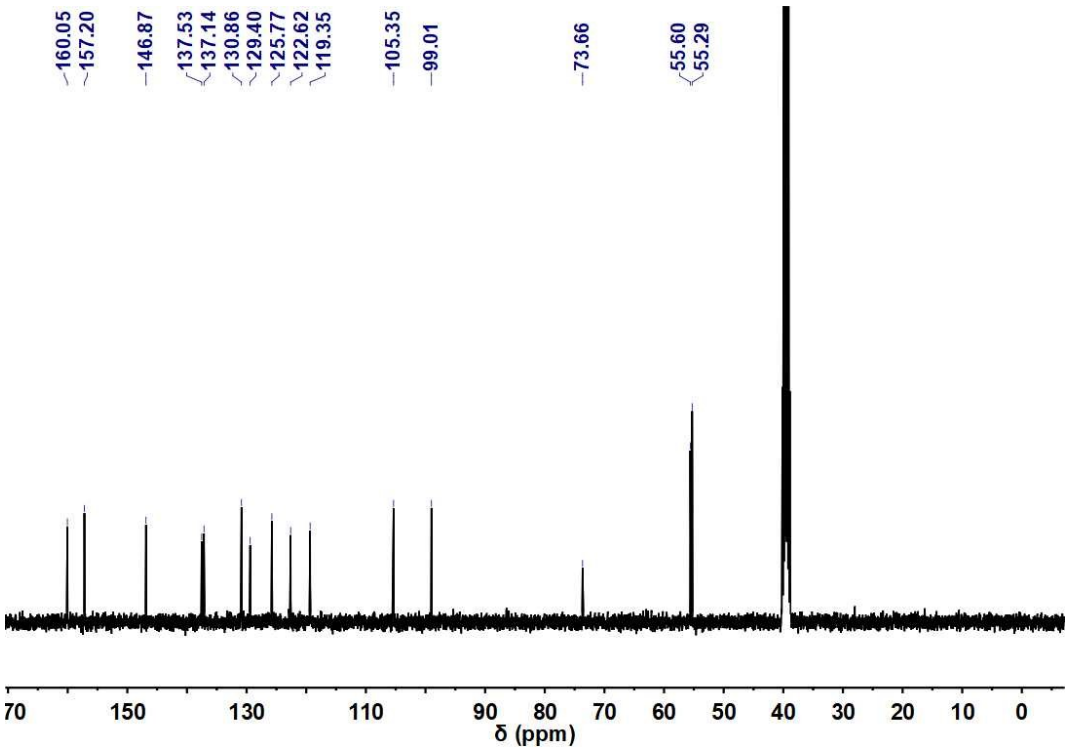

Figure S12. [13]C NMR spectrum (100 MHz, DMSO-d_6, 298K) of **MOH**.

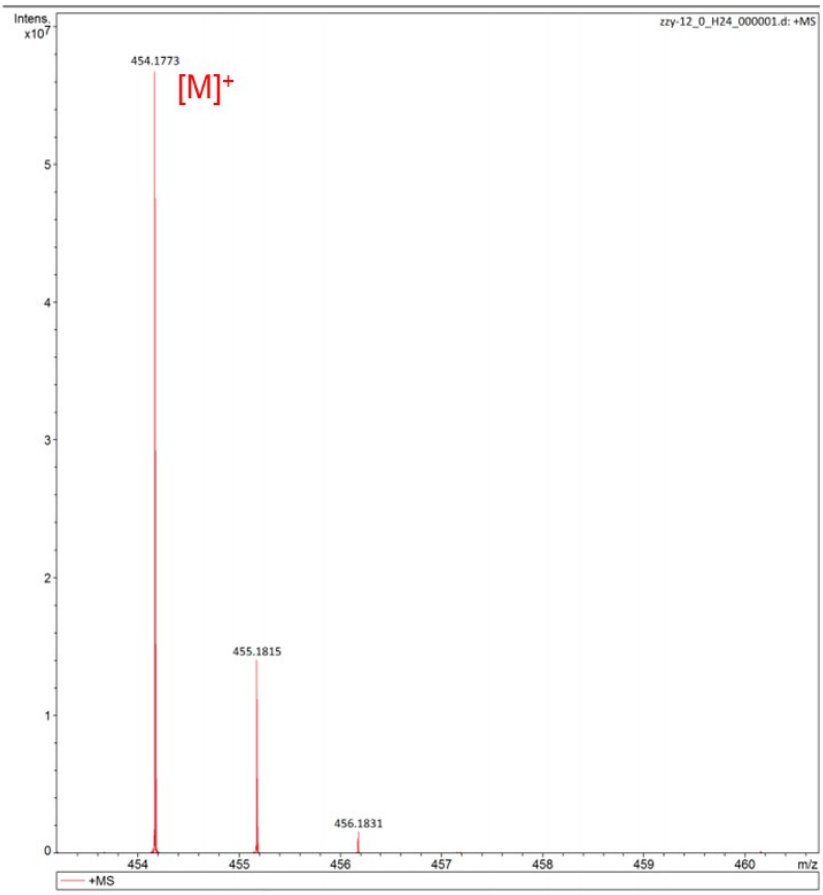

Figure S13. HRMS of **MOH**.

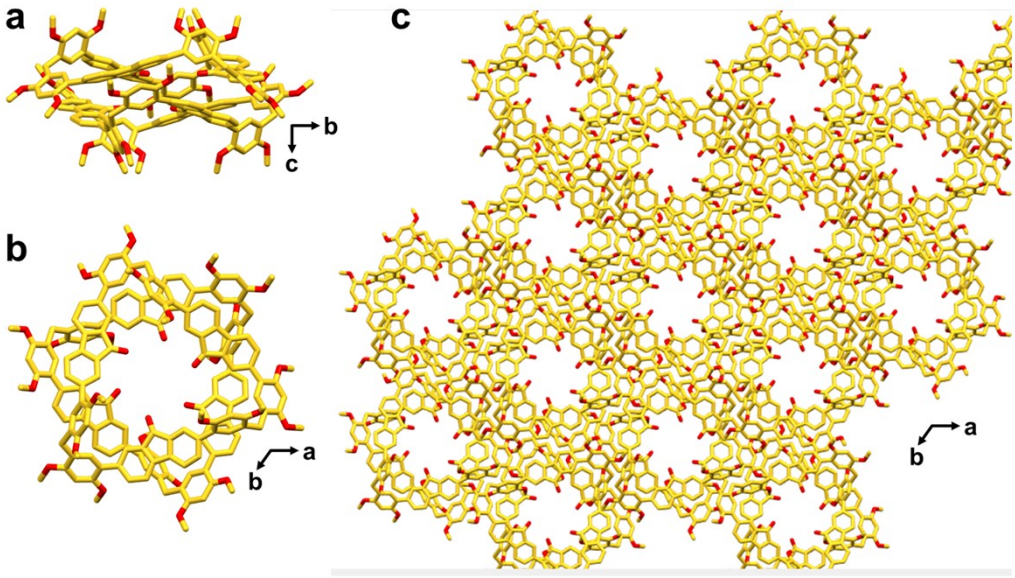

Figure S14. Single-crystal structures and superstructures of **T1OH** view along (a) a axis and (b, c) c axis. Hydrogen atoms are omitted for the sake of clarity.

Table S4. Crystal data of **T1OH**.

CCDC	2193451
Name	**T1OH**
Empirical formula	$C_{102}H_{92}N_6O_{15}$
Formula weight	1641.81
Temperature / K	100.00 (10)
Radiation / Å	CuKα
	(λ= 1.54184)
Crystal system	trigonal
Space group	R -3
a / Å	31.2235(3)
b / Å	31.2235(3)
c / Å	15.7464(10)
α / °	90
β / °	90
γ / °	120
Volume/ $Å^3$	13294.6(3)
Z	6
Density (calculated)	1.230 g/cm^3
μ / mm^{-1}	0.669
F(000)	5196.0
Crystal size (mm^3)	0.2×0.15×0.1
2θ range /°	13.012 to 151.498
Index ranges	$-30 \leqslant h \leqslant 30$
	$-37 \leqslant k \leqslant 37$
	$-18 \leqslant l \leqslant 18$
Reflections collected	18893
Independent reflections	5833
R(int)	0.0232
Data/restraints/parameters	5833/9/376
Goodness-of-fit on F^2	0.971
Final R indices [I>2sigma(I)]	R_1 = 0.0374
	wR_2 = 0.1037
Largest diff. peak/hole / e $Å^{-3}$	1.38/-0.70

Section III. Photophysical properties

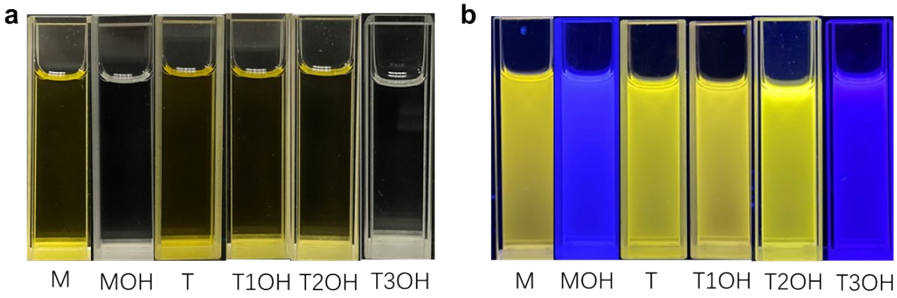

Figure S15. Pictures of **M**, **MOH**, **T**, **T1OH**, **T2OH** and **T3OH** in THF at (a) day light and (b) 365 nm UV lamp.

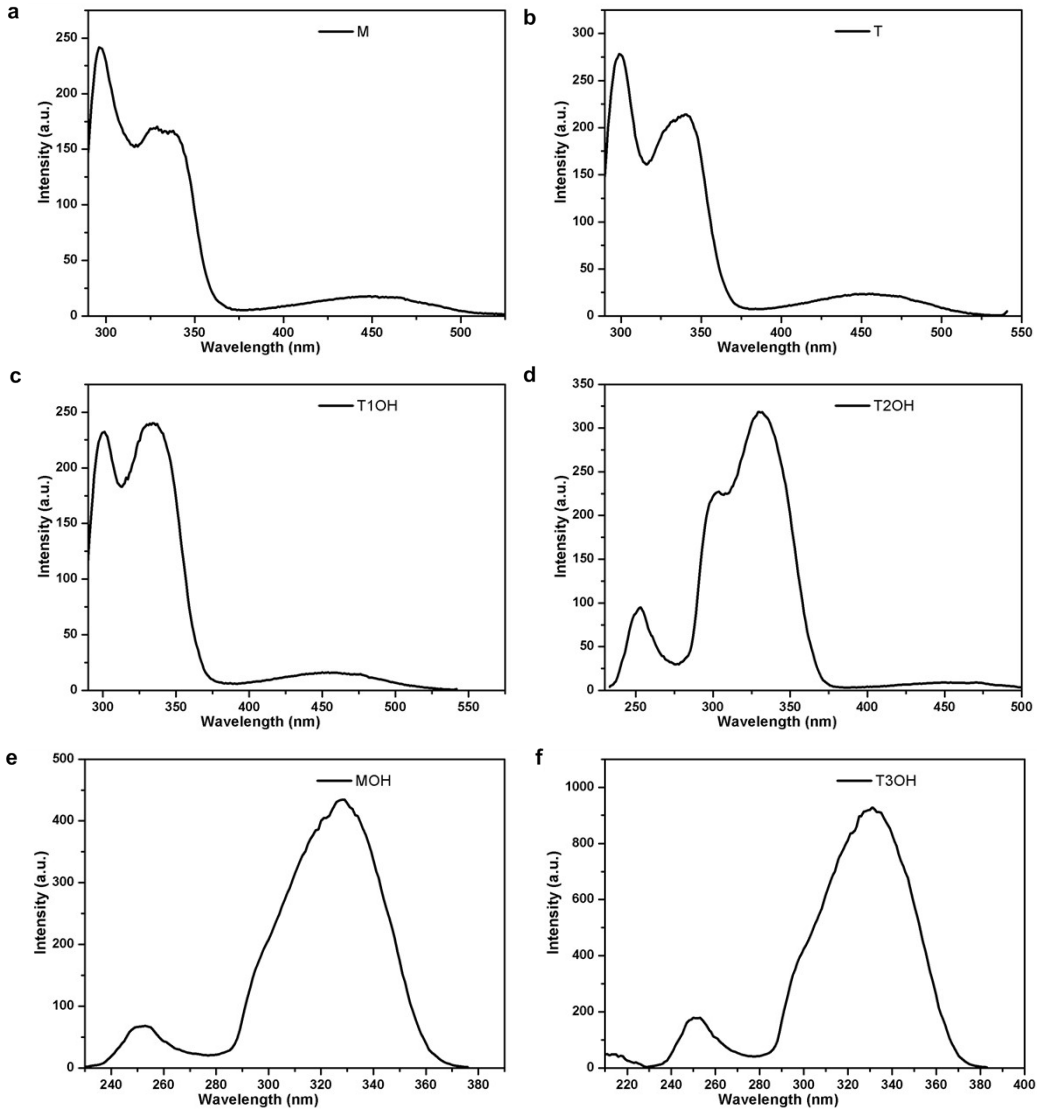

Figure S16. Excitation spectra of (a) **M** (@538 nm), (b) **T** (@550 nm), (c) **T1OH** (@552 nm), (d) **T2OH** (@547 nm), (e) **MOH** (@386 nm) and (f) **T3OH** (@393 nm) in THF solution (1×10^{-6} mol/L).

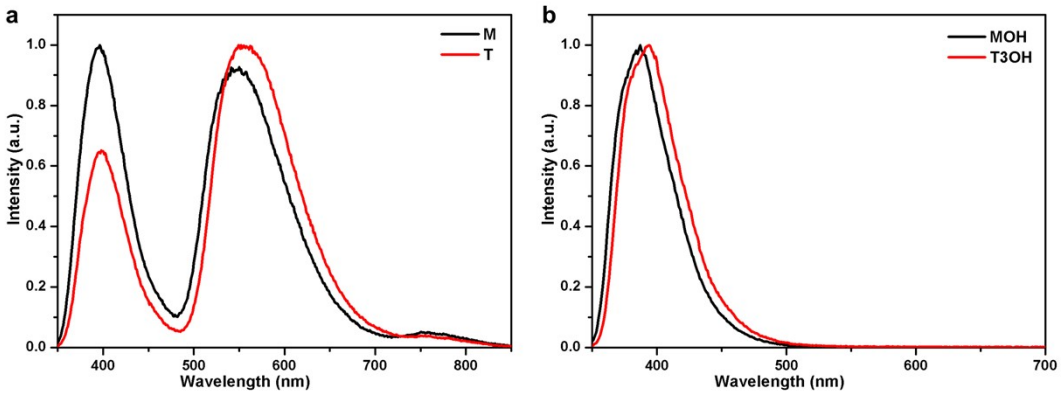

Figure S17. Normalized photoluminescence spectra of (a) **M** and **T** and (b) **MOH**, and **T3OH** in THF solution (1×10^{-6} mol/L).

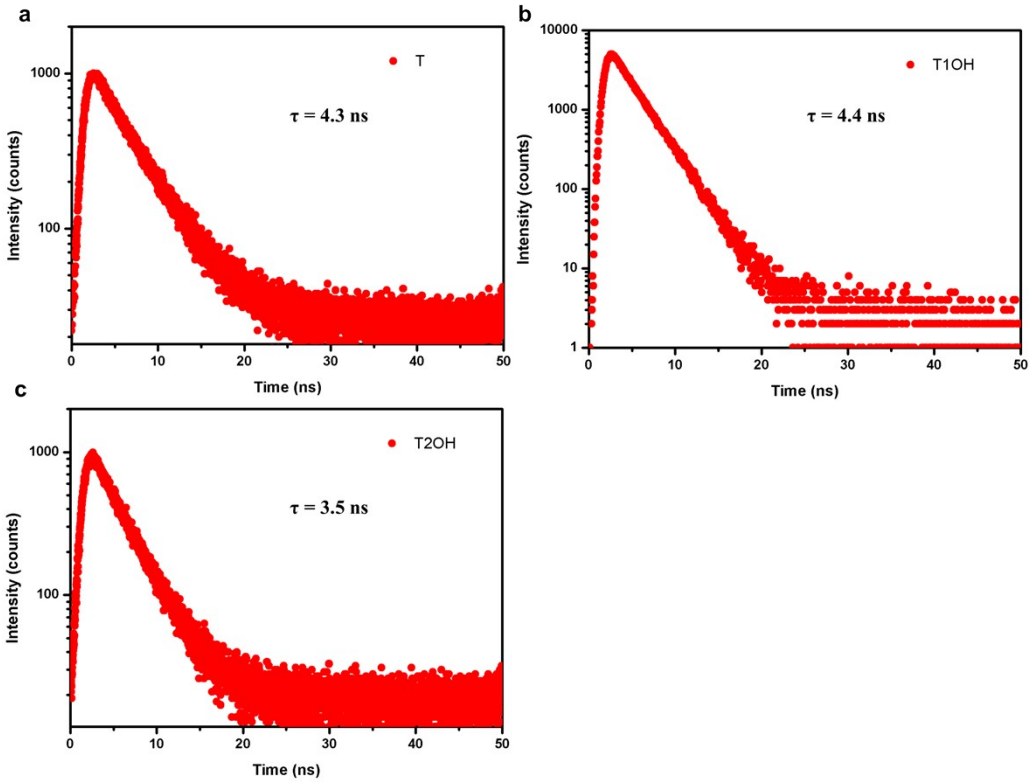

Figure S18. Time-resolved PL decay of **T**, **T1OH**, and **T2OH** in THF solution at 554 nm (1×10^{-6} mol/L).

Table S5. Photophysical data of **T**, **T1OH**, **T2OH** and **T3OH** in solution and in solid state.

Entry	Compound	λ_F (nm)	τ_F (ns)	Φ_F (%)	$K^F_{r(s^{-1})}$ [c]	$K^F_{nr(s^{-1})}$ [d]
1	**T** (L) [a]	554	4.3	5.4	1.25×10^7	2.20×10^8
2	**T1OH** (L) [a]	554	4.4	4.5	1.03×10^7	2.17×10^8
3	**T2OH** (L) [a]	554	3.5	8.0	2.31×10^7	2.63×10^8
4	**T3OH** (L) [a]	393	1.3	40.0	3.10×10^8	4.62×10^8
5	**T** (S) [b]	580	3.4	1.6	4.74×10^6	2.89×10^8
6	**T1OH** (S) [b]	580	1.9	4.0	2.10×10^7	5.05×10^8
7	**T2OH** (S) [b]	580	2.3	1.4	5.98×10^6	4.27×10^8
8	**T3OH** (S) [b]	393	7.7	4.2	5.44×10^6	1.24×10^8

a: In THF solution. b: In solid state. c: The radiative decay rate constant of fluorescence $k^F_r = \Phi_F/\tau_F$.

d: The nonradiative decay rate constant of fluorescence $k^F_{nr} = (1- \Phi_F - \Phi_P)/\tau_F$, $\Phi_P = 0$.

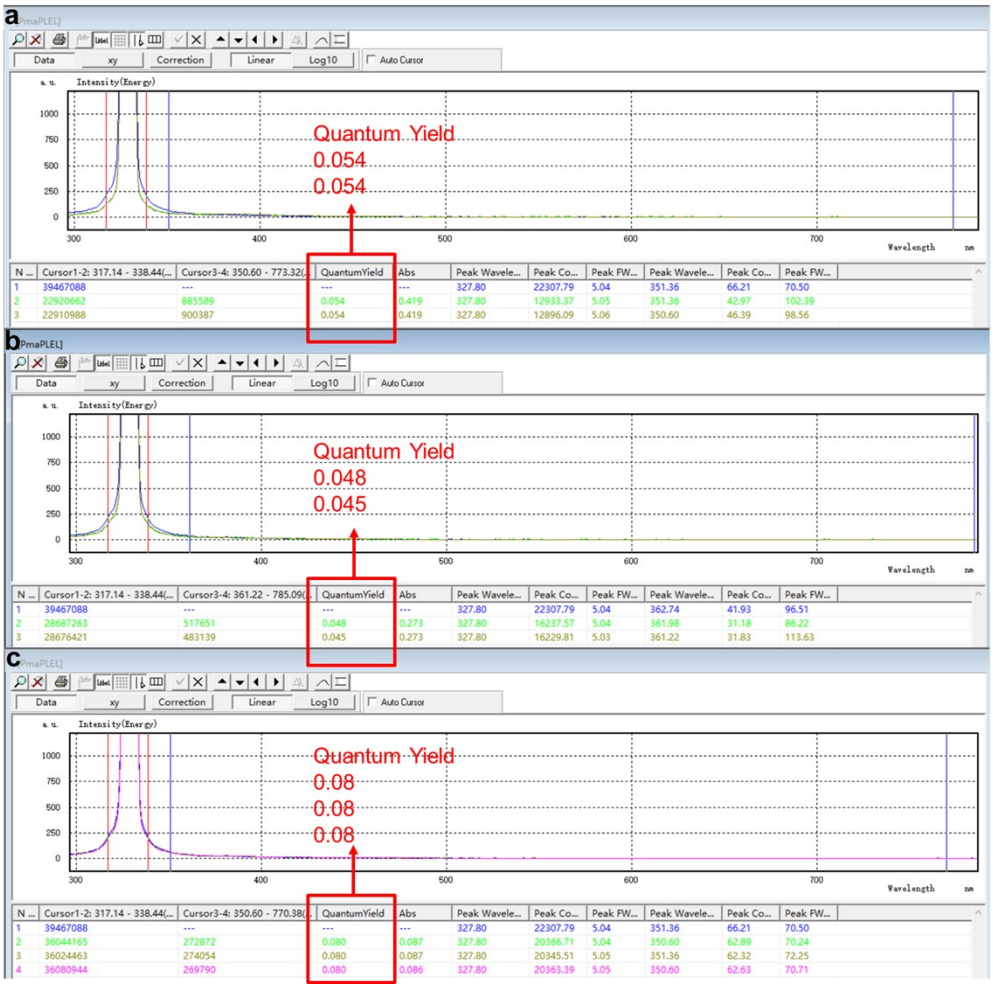

Figure S19. Quantum yields of fluorenone moiety in (a) **T**, (b) **T1OH**, and (c) **T2OH** in THF solution (1×10^{-6} mol/L).

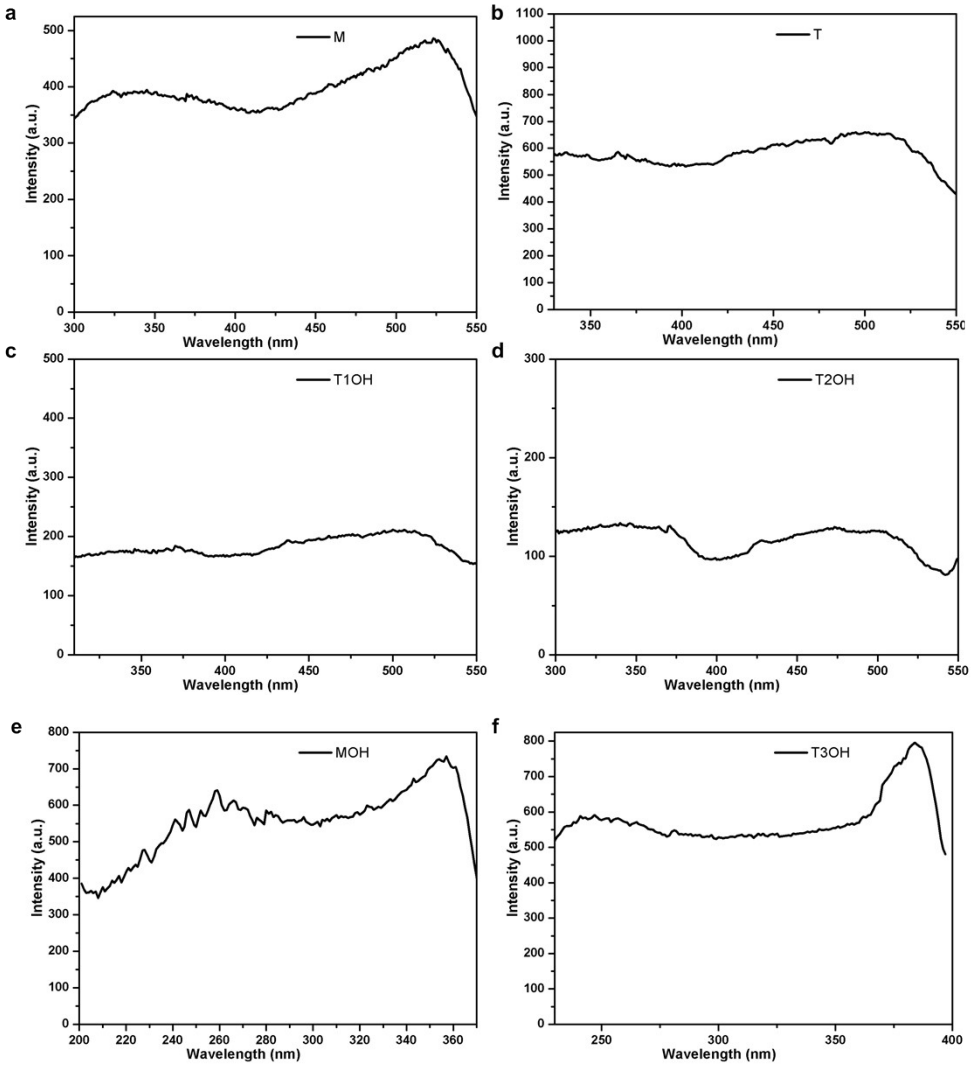

Figure S20. Excitation spectra of (a) **M** (@576 nm), (b) **T** (@588 nm), (c) **T1OH** (@ 596nm), (d) **T2OH** (@579 nm), (e) **MOH** (@382 nm), and (f) **T3OH** (@407 nm) in solid state.

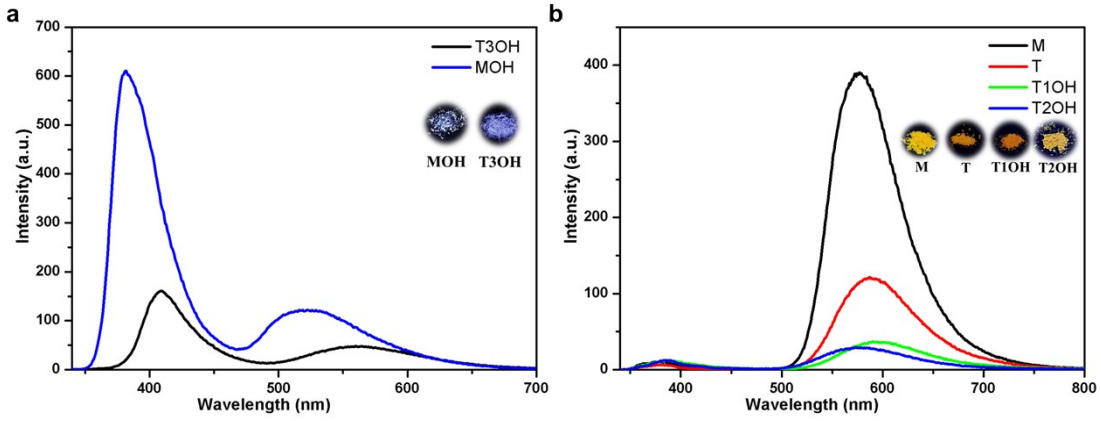

Figure S21. (a) Photoluminescence spectra of **MOH** and **T3OH** in solid state. (b) Photoluminescence spectra of **M**, **T**, **T1OH**, and **T2OH** in solid state.

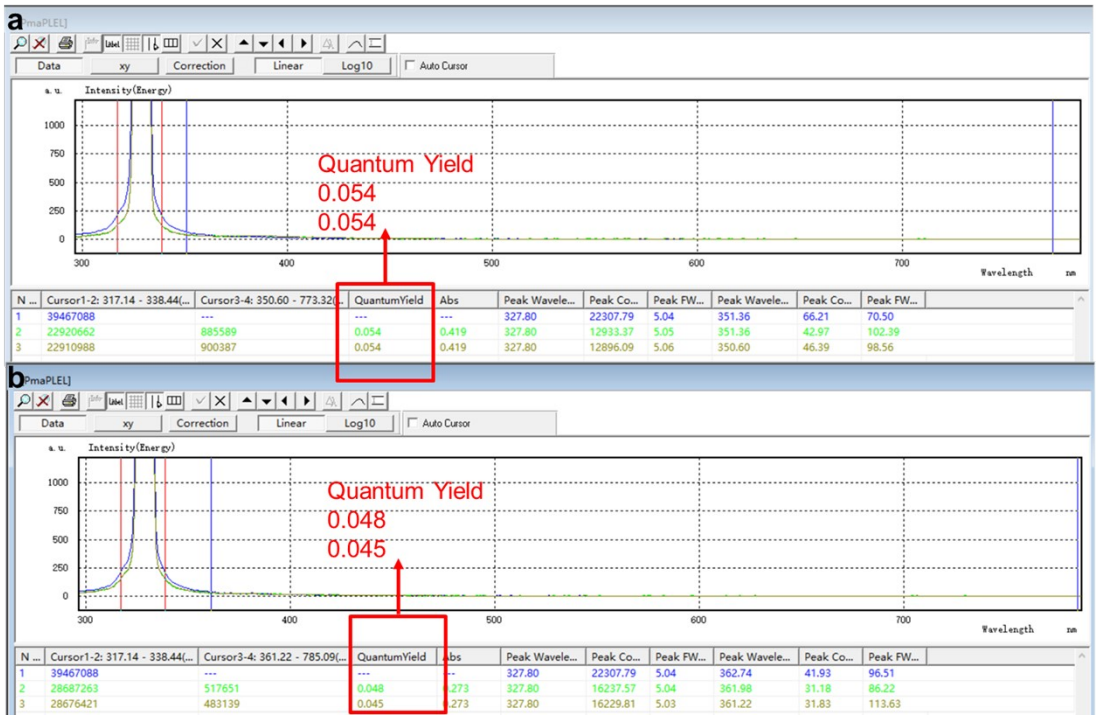

Figure S22. Quantum yields of (a) **T** and (b) **T1OH** in 1×10^{-6} mol/L THF solution.

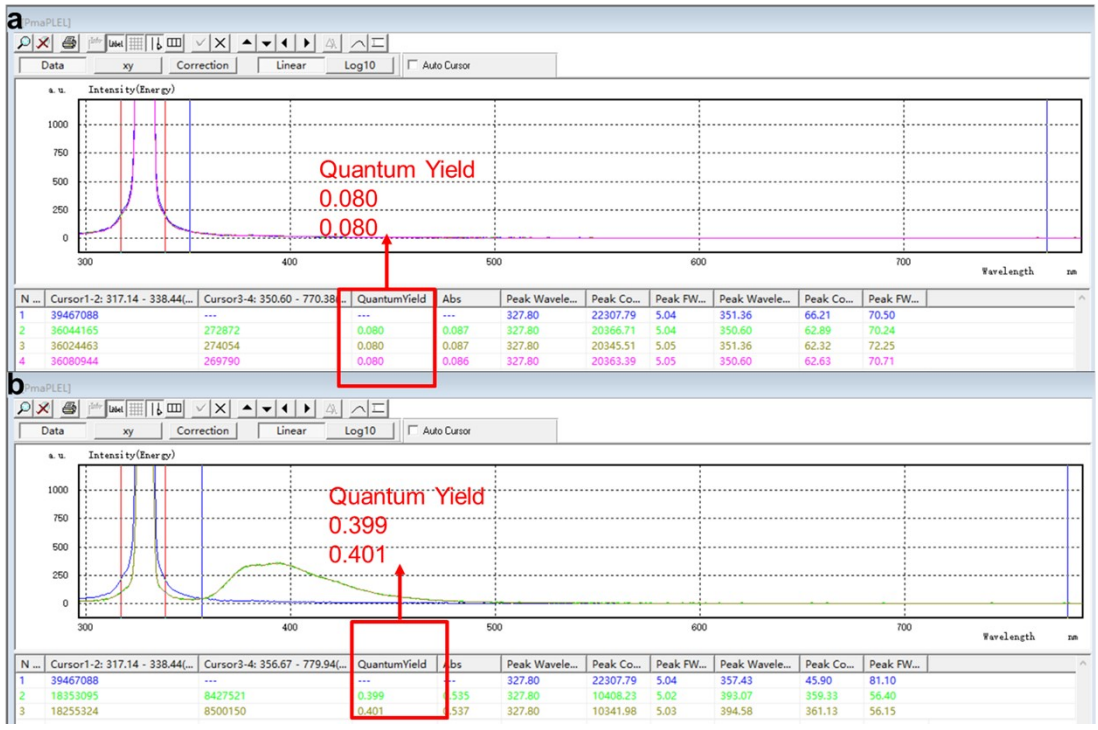

Figure S23. Quantum yields of (a) **T2OH** and (b) **T3OH** in THF solution (1×10^{-6} mol/L).

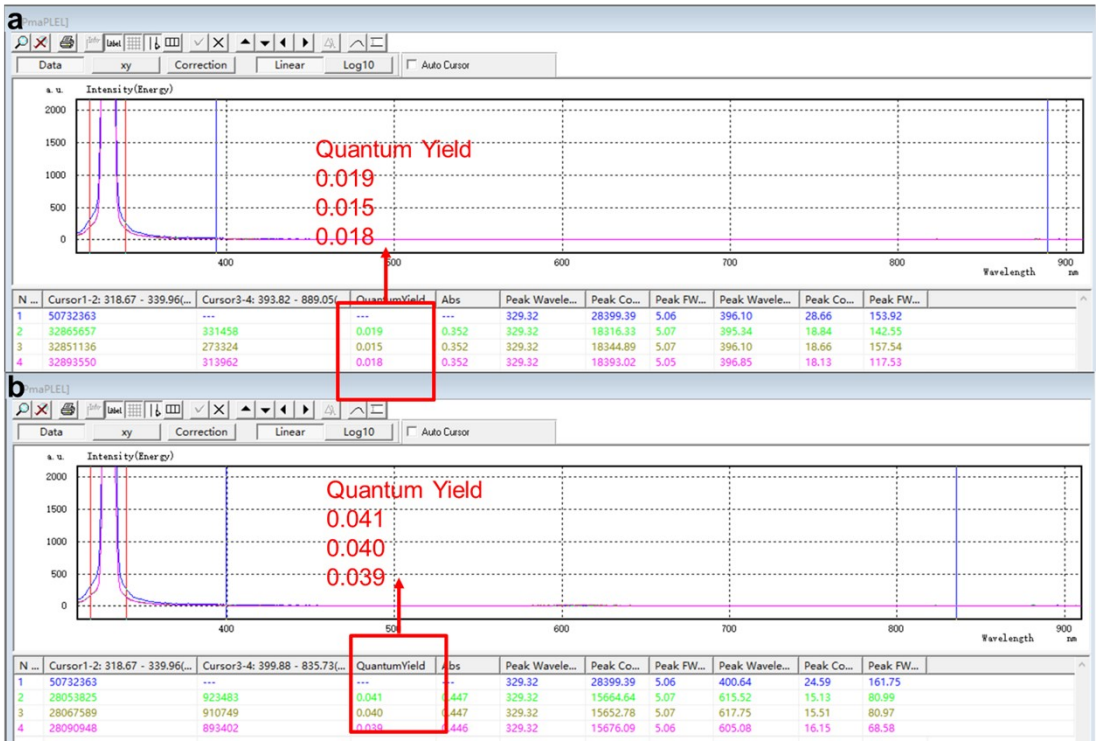

Figure S24. Quantum yields of (a) **T** and (b) **T1OH** in solid state.

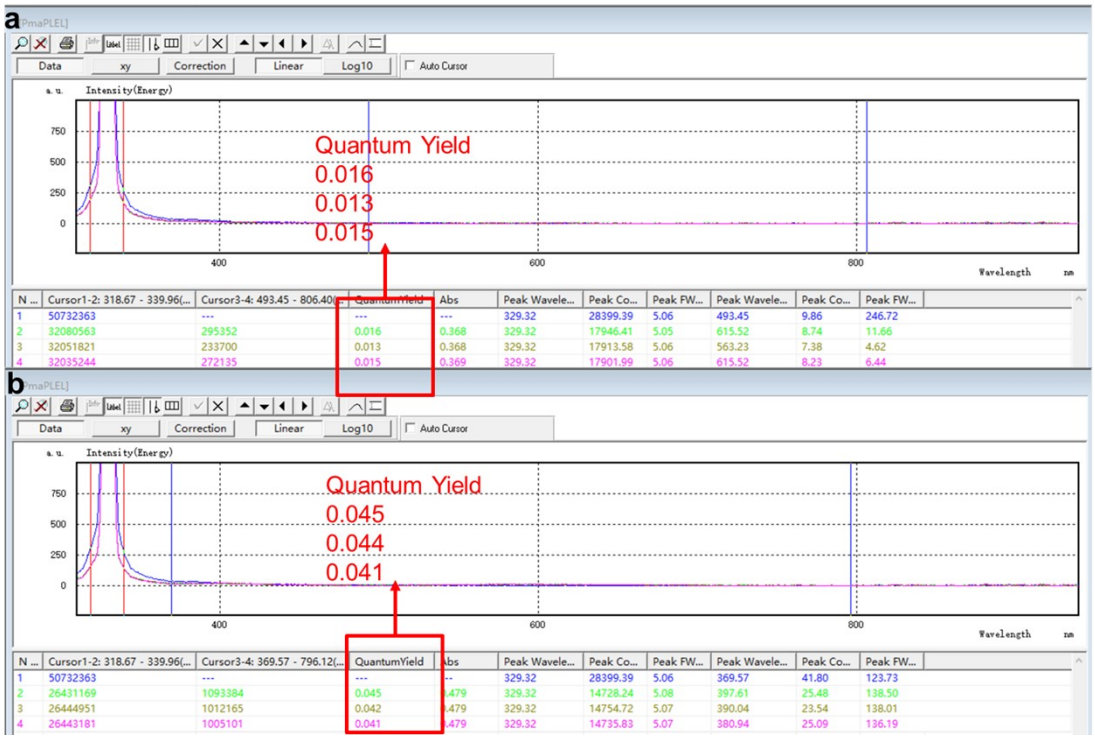

Figure S25. Quantum yields of (a) **T2OH** and (b) **T3OH** in solid state.

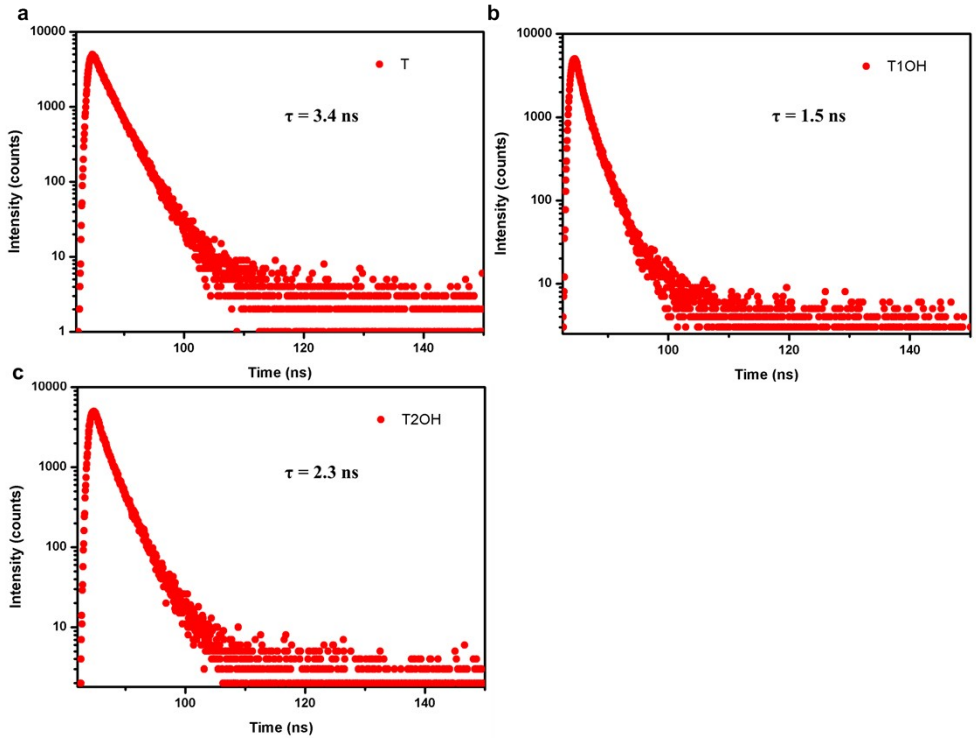

Figure S26. Time-resolved PL decay of **T**, **T1OH**, and **T2OH** in solid state at room temperature (@580nm).

References:

[1] MOPAC2016, James J. P. Stewart, *Stewart Computational Chemistry*, Colorado Springs, CO, USA, **2016**, HTTP://OpenMOPAC.net.

[2] Stewart J. J. P., Optimization of parameters for semiempirical methods VI: more modifications to the NDDO approximations and re-optimization of parameters. *J. Mol. Modeling.* **2013**, *19*, 1-32.

[3] Behzad, Z.; Tarifeh, B. Wet THF as a Suitable Solvent for a Mild and Convenient Reduction of Carbonyl Compounds with NaBH4. Bull. Chem. Soc. Jpn. **2005**, 78, 307-315.

[4] Gao, B.; Tan, L.-L.; Song, N.; Li, K.; Yang, Y.-W. A high-yield synthesis of [m]biphenyl-extended pillar[n]arenes for an efficient selective inclusion of toluene and m-xylene in the solid state. *Chem. Commun.* **2016,** *52*, 5804-5807.

[5] Zhang, Z.; Luo, Y.; Chen, J.; Dong, S.; Yu, Y.; Ma, Z.; Huang, F. Formation of Linear Supramolecular Polymers That Is Driven by C□H···π Interactions in Solution and in the Solid State. *Angew. Chem. Int. Ed.* **2011,** *50*, 1397-1401.

[6] Boinski, T.; Szumna, A. Hybrid[4]arenes with anthracene units and tuneable cavities. *New J. Chem.* **2017,** *41*, 3387-3391.

[7] Zhang, Z.; Xia, B.; Han, C.; Yu, Y.; Huang, F. Syntheses of Copillar[5]arenes by Co-oligomerization of Different Monomers. *Org. Lett.* **2010,** *12*, 3285-3287.

[8] Xu, K.; Zhang, Z.-Y.; Yu, C.; Wang, B.; Dong, M.; Zeng, X.; Gou, R.; Cui, L.; Li, C. A Modular Synthetic Strategy for Functional Macrocycles. *Angew. Chem. Int. Ed.* **2020,** *59*, 7214-7218.

[9] Zhou, J.; Yang, J.; Hua, B.; Shao, L.; Zhang, Z.; Yu, G. The synthesis, structure, and molecular recognition properties of a [2]calix[1]biphenyl-type hybrid[3]arene. *Chem. Commun.* **2016,** *52*, 1622-1624.

[10] Boinski, T.; Cieszkowski, A.; Rosa, B.; Szumna, A. Hybrid [n]Arenes through Thermodynamically Driven Macrocyclization Reactions. *J. Org. Chem.* **2015,** *80*, 3488-3495.

[11] Li, J.; Han, X.-N.; Zhou, H.-Y.; Han, Y.; Chen, C.-F. Helic[1]triptycene[3]arene: Synthesis, Complexation, and Formation of [2]Rotaxane Shuttle. *J. Org. Chem.* **2020,** *85*, 11465-11474.

[12] Boinski, T.; Cieszkowski, A.; Rosa, B.; Leśniewska, B.; Szumna, A. Calixarenes with naphthalene units: calix[4]naphthalenes and hybrid[4]arenes. *New J. Chem.* **2016,** *40*, 8892-8896.

[13] Yu, C.-M.; Meng, X.; Liu, X.; Zhang, Z.-Y.; Li, C. Switchable Supramolecular Jalousie Constructed from a Fluorenone Macrocycle. *Chem. Mater.* **2022,** 34, 358-365.